2018 7th IEEE International Conference on Biomedical
Robotics and Biomechatronics (Biorob)
Enschede, The Netherlands, August 26-29, 2018

Examining the Impact of Wrist Mobility on Reaching Motion Compensation across a Discretely Sampled Workspace

Adam J. Spiers, *Member, IEEE,* Yuri Gloumakov and Aaron M. Dollar, *Senior Member, IEEE*

***Abstract*— This paper presents an effort to characterize the impact of wrist mobility on reaching motion compensation over an evenly sampled planar workspace. When the degrees of freedom of the arm are limited due to injury or amputation, the behavior of other joints is modified to achieve the same motion goals. Though several past studies have measured motion compensation for simulated activities of daily living, the results tend to be specific to one spatial configuration of user and objects. Conversely, this paper aims to understand how motions and compensation vary when the same task (reaching-and-grasping) is conducted at a variety of locations across in the workspace. This high-resolution sampling enables spatial patterns of unimpaired and impaired movement to be identified. To achieve this, joint angles and Cartesian trajectories of the upper body were recorded as able-bodied participants reached and grasped 49 (7×7) equally spaced vertical cylindrical targets on a 1.9×1.9m grid, using their dominant hand. This was first completed naturally and then while wearing a custom orthopedic arm brace, which limits all 3DOF (degrees of freedom) of wrist motion. Each reaching motion was segmented and independently analyzed using metrics for range of motion, and Cartesian path length of body segments. A spatial 'heat-map' display approach visually indicates how regions of the workspace affect the behavior of different body joints and segments. Further statistical analysis quantifies these visual trends. The results indicate wrist mobility has significant impact on shoulder and elbow ROM in addition to the length of Cartesian motion trajectories for the wrist and elbow.**

I. Introduction

Developments in the field of upper limb prosthetics often focus on creating more dexterous prosthetic terminal devices, to replace the absent hands of amputees and facilitate object holding and grasping. This is demonstrated by the wide range of anthropomorphic prosthetic hands generated by industry (e.g. [1]), academia and hobbyists (e.g. [2]). In comparison, there has been fairly little attention given to the development of prosthetic wrists [3], despite the fact that this part of the body is also absent in many amputees. It is common for above-wrist amputees to be fitted with prosthetic devices that either have no wrist, or only a passive pronation/supination mechanism that must be rotated by the other limb or some environmental feature. This effectively fixes the alignment of their prosthetic device with regard to their forearm.

Such an absence of wrist mobility limits the orientation capability of the hand relative to the body. In order to achieve the same target hand orientations necessary for grasping a variety of objects, it is necessary to modify the motion trajectories of other joints. This leads to compensatory movements, which can place additional stress on the body and lead to overuse complications for the remaining joints [4], [5]. An example compensatory motion for a trans-radial amputee involves elevating the elbow while drinking, to facilitate the tipping of mug or bottle to the mouth, an action that is usually carried out by the wrist. This action increases shoulder motion to compensate for the lack of wrist mobility.

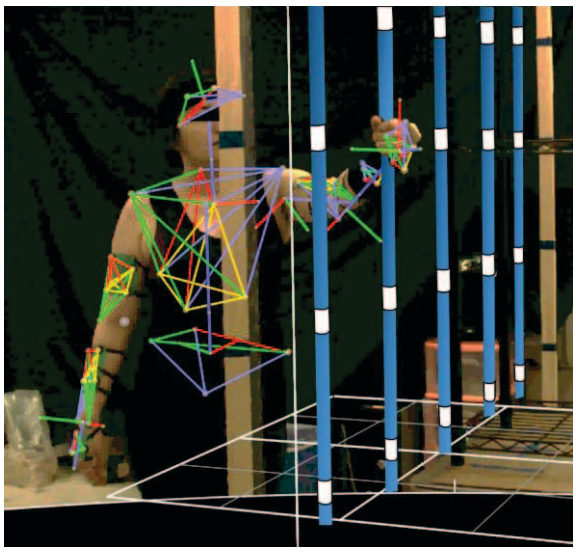

Figure 1. A participant reaching to one of the 49 targets on the grid. Their motion capture 'skeleton' has been overlaid, illustrating co-ordinate frames of their trunk and dominant (left) arm. Five of the seven vertical poles have been coloured blue to improve visibility in this image (their actual color is black, to reduce reflectivity).

The importance of the wrist for appropriately positioning the hand has been highlighted in work such as [4]. Here the authors argue that coupling a simple gripper with a dexterous wrist could be more effective for aiding manipulation than the current practice of fitting dexterous multi-grasp prosthetic hand to sockets without wrists. It should be noted however that prosthetic wrist technology is still limited in terms of capability, and that issues of controlling multi-DOF wrists have yet to be adequately addressed [3].

Compensatory motions have been previously studied by various groups for various medical conditions [4]–[7]. These studies all involved ADL (activities of daily living) tasks such as preparing food, lifting an object or completing tasks from a standardized hand function outcome measure (e.g. the SHAP

* Research supported by the Telemedicine & Advanced Technology Research Center (TATRC) US Army Medical Research & Materiel Command

A. J. Spiers is with the Department of Haptic Intelligence, Max Planck Institute for Intelligent Systems, Stuttgart, 70597, Germany.

Y. Gloumakov and A. M. Dollar are with the Department of Mechanical Engineering, Yale University, New Haven, CT 06511, USA. (phone: +49-711-689-2003, e-mail: a.spiers@is.mpg.de, yuri.gloumakov@yale.edu, aaron.dollar@yale.edu).

978-1-5386-8183-1/18/$31.00 ©2018 IEEE

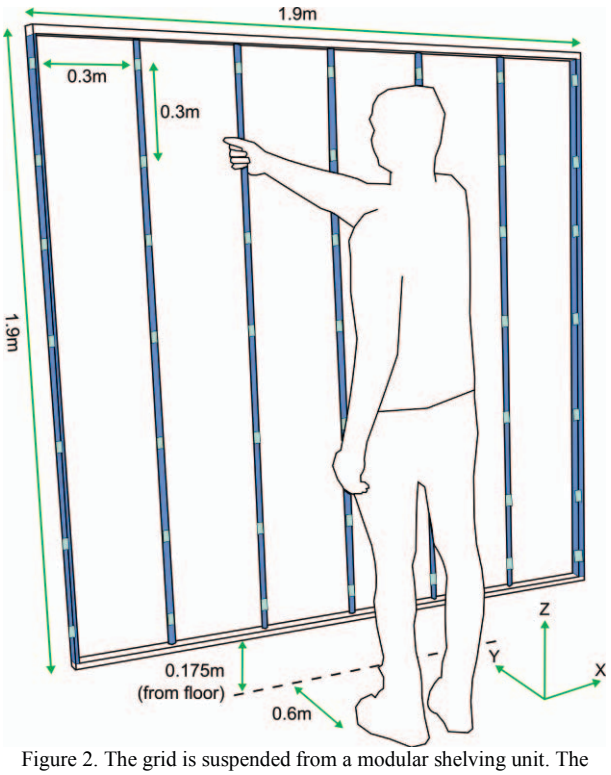

Figure 2. The grid is suspended from a modular shelving unit. The vertical poles and wooden outer supports of the grid feature reaching targets (indicated with tape). Targets have 0.3m seperation in vertical and horizontal directions. The global co-ordinate axis are shown.

test). In this work, we wish to build upon these studies by proposing the characterization of motion compensation over a user's workspace via discrete sampling. Similar approaches have been applied to modelling parameters across the workspace of simple robot manipulators [8]. Our goal in this work is to understand and quantify how different regions of a user's workspace impact compensatory motions in different joints of the body.

In this paper we introduce a method of studying compensatory motions across a user's workspace with a semi-abstract reaching task. We use an equally spaced 7x7 grid of vertically orientated cylindrical targets to simulate the grasping of common objects (e.g. cups, cans, etc.) at various heights and lateral displacements from a participant's body (Fig 1 and Fig 2). A Vicon motion capture system enables recording of body motion for the reaching actions necessary to grasp each target, thereby allowing characterization of the workspace with respect to a variety of metrics. Reaching to objects at various locations in a workspace is a common manipulation scenario that may be found in many kitchen, wardrobe or supermarket settings (Fig 3). These environments are associated with eating, dressing and shopping, which are beneficial for personal independence. In this study, participants reach to all points on the grid unimpaired and whilst wearing a custom device to brace wrist motion.

Reaching motions and joint trajectories are known to be similar within and across unrestrained healthy participants [9], [10], though error bounds are visible in joint-angle measurements (e.g. [7]). To allow better interpretation of this similarity, we present a 'heat-map' based representation of various metrics. We also provide a statistical method to allow

Figure 3. Supermarket shelving is a common environment that requires reaching to multiple target locations in an individual's workspace (image from Alamy.com)

between subjects comparison of the resulting data, highlighting which joints have similar patterns of compensation across participants.

II. Related Work

Various groups have highlighted and made efforts to quantify compensatory motion in persons with impaired wrist mobility (e.g. [4]–[7], [11]–[14]). A common protocol in these studies involves participants performing simulated ADLs, while under observation from a motion capture system. Often, the Range Of Motion (ROM) of a joint is calculated for different study conditions [4]–[7], [11], though other metrics, such as mean angle [14], have been applied.

The SHAP (Southampton Hand Assessment Protocol) [15] test has featured in a variety of motion studies, due to its standardized simulated ADLs, which explore different grasps and manipulation capabilities. In [7] the page-turning task of the SHAP test was used to compare the joint motions of unimpaired participants with those who had previously experienced a wrist injury. Joint ROM comparisons illustrated that impaired participant joint motion was often outside of the typical range of uninjured participants.

In [5] able bodied and amputee prosthesis-users performed a number of ADL tasks while their trunk and head motions were measured, with increased ROM identified in the prosthesis users. A similar study measured trunk, shoulder and elbow ROM during selected SHAP test tasks [11].

To enable the study of body compensation within-subjects, wrist splints (which limit flexion/extension, radial/ulnar deviation and partially limit pronation/supination) were used to constrain participant wrist mobility in [4], [13], [14]. In [4], participants performed tasks from the SHAP test while their wrist or finger motion was restricted. ROM was reported for trunk and shoulder angles. An alternative outcome measure, the Jebsen test, was used as the basis of participant motion in [13]. Only a limited number of forearm, elbow and shoulder and trunk motion differences were statistically significant for particular tasks. However, participants did report more impairments in self-reporting surveys. In [14], the task was limited to removing an object from a box. Mean joint angles were calculated with/without a wrist splint as a measure of compensatory motion.

A goal of studying the body compensation that stems from wrist impairment is to better inform the design/choice of new prosthetic devices and interventions. Indeed, this approach was taken in [6], where different prosthetic wrist modules were evaluated in amputees. Shoulder joint angles were considered representative of compensatory motion, though no statistically significant difference was noted between the wrist modules.

III. Methods

A. Study Apparatus

The study involved participants reaching to a set of 49 target locations equally spaced across a 7x7 grid (Fig 2). The grid was constructed from a wooden frame with five plastic PVC pipes reaching between its top and bottom edges. The pipe was wrapped in black matt tape to minimize reflections in the optical motion capture environment. Blue tape was wrapped around these pipes and wooden structures in specific locations to create reaching targets that participants were required to grasp. The vertical cylindrical nature of the targets provides similarities to grasping common objects like cups, bottles and tins from shelves in a kitchen or supermarket.

The grid measures 1.9x1.9m at its outermost edges. The vertical pipes have a diameter of 25mm and the wooden frame members have a cross section of 20x30mm. Targets are spaced at 0.3m intervals horizontally and vertically. The grid is suspended from a modular shelving unit, so that the base of the grid is suspended 0.175m off the ground. Participants stand 0.6m from the grid, with their torso laterally aligned with the central pole. Marks on the floor help participants stay aligned during the study.

The grid is in the center of a symmetrical arrangement of 12 Vicon *Bonita* motion capture cameras arranged at different heights. An additional video reference camera is connected to the Vicon system (Fig 1 was produced with this camera).

Participants wore retroreflective motion capture markers on their pelvis, torso, head and arms in line with the recommendations of the International Society of Biomechanics (shoulder co-ordinate system 2) [16], which are also reflected in [7]. Torso markers were attached to a sleeveless skin-tight (Nylon/Lyrca blend) sports shirt (which was available to participants in various sizes), while head markers were affixed to an elastic sports headband. Other markers were attached directly to the skin with double-sided adhesive tape. In addition, three marker 'clusters' were worn on each arm (on the humerus, forearm and back of the hand), as illustrated in Fig 1. The clusters are constructed from thin flexible plastic which are strapped to the user's body with elastic straps. A piece of double-sided tape underneath each cluster prevented it from slipping against the wearer's skin. While the skin based markers mainly contributed to joint angle calculation, the clusters were used for reconstructing markers whose tracking was lost by the Vicon system. Such loss was common, due to the large motion ranges and workspace of this study. In post-processing, joint angles of the trunk, shoulder, elbow and wrist were calculated via the methods of [16].

To impair wrist motion on the participant's dominant arm, a padded orthopedic wrist brace featuring an aluminum internal structure (DonJoy ComfortFORM Wrist Support Brace – DJO Global, Vista CA, USA) was combined with a padded elbow brace with elbow articulation (Orthomen ROM Elbow Brace) by means of a bolt. An additional wooden insert was added to this setup to prevent wrist extension (Fig 4). In all, this combination of orthotic devices effectively limited wrist pronation/supination, radial/ulnar deviation and wrist flexion/extension. Note that the majority of previous work in this area have used wrist brace that do not limit pronation/supination [4], [13], [14]. Note also that though the Elbow brace has the ability to restrict elbow range of motion, the device was set to allow a user's full range of elbow motion. It's primary function was to limit pronation/supination.

Figure 4. A custom bracing system was created for this study by combining an commerical elbow brace with a wrist orthosis, modificed with an additional wooden insert to limit wrist flexion/extension. This arrangment limits motion of all 3DOF of the wrist.

B. Study Procedure

This study procedure has been approved by the Yale University IRB office, protocol number #HSC 1610018511.

Participants stood on marks made on the floor at a distance of 0.6m from the grid. They were requested to reach to each target on the grid, forming a power grasp and squeezing the target. Following each target they were asked to return to a relaxed position with arms by their sides. Targets were completed one row at a time, in a right to left order, starting with the top right target. Participants were requested to only step away from the start position on the floor if necessary to reach a target and to return to the start position after each grasp. If participants failed to return to the start position for a target then the reaching motion was repeated for that target.

Participants completed the grid reaching task as part of a larger battery of tasks, the data from which is being used for various studies. The additional tasks involved various ADL activities and standardized outcomes measures. It took approximately 30 minutes to affix markers to participants and calibrate the motion capture system. The actual grid reaching procedure took approximately 20 minutes. Participants were reimbursed financially for their involvement.

C. Participants

Four participants (Table 1) took part in this initial run of the study, with the addition of further participants planned for

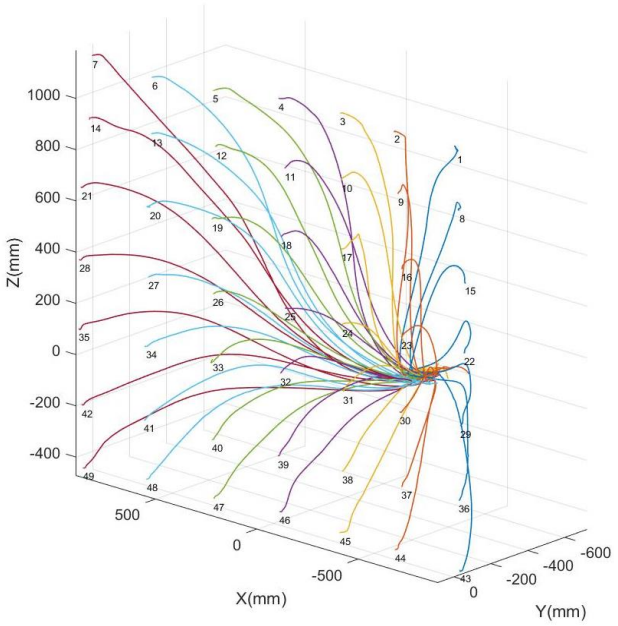

Figure 5. Segmented unimpaired wrist center (C_{WR}) reaching trajectories for participant P2, showing 49 motions.

future work. All participants completed an initial screening to confirm that they did not suffer from any motion impairments.

IV. Data Processing

A. Data structure

Marker data was processed using Vicon Bodybuilder and custom Matlab code (based on [16]) to create co-ordinate frames at the center of the wrist, elbow and shoulder of the dominant arm. Additional co-ordinate frames were also created for the pelvis, thorax and head. These frames enabled the extraction of joint angles θ and Cartesian position data C.

B. Segmentation

Reaching data for all targets was recorded in a single Vicon trial for each study condition (with or without arm bracing). This data was then segmented in Matlab based on the lateral position the wrist perpendicular to the plane of the grid (the Y axis in Fig 2). Superfluous motions (such as repeating targets, swinging the arm or scratching the body) were manually removed. Only motions recorded during reaching towards the grid were retained for further analysis. These motions, for the wrist center only (C_{WR}), are shown for P2 in Fig 5.

C. Metrics

Several motion metrics were considered for analysis of the captured data, as it was observed that particular variations in reaching patterns may not be captured by a single metric. Fig 6 illustrates trajectories of two joints for participants P1 and P2 in unimpaired and impaired cases. The typical measures of joint ROM will show differences between the impaired and unimpaired conditions for the trunk case. However, little difference would be indicated for the shoulder case. This is despite a large trajectory divergence in the middle of the motion for P1. Following these considerations, the metric of ROM was combined with Cartesian trajectory length when evaluating the motion data.

Table 1. Characteristics of the four participants. Weight is in lbs. 'Dom. Hand' is an abbreviation of dominant hand. Arm length is measured from the shoulder to the tip of the middle finger.

Participant	Sex	Age	Weight	Height	Dom. Hand	Arm Length
P1	F	24	125	5'6.5"	R	28"
P2	M	29	185	6'2"	R	27"
P3	M	24	160	5'8"	R	24"
P4	M	54	175	5'10"	R	27.5"

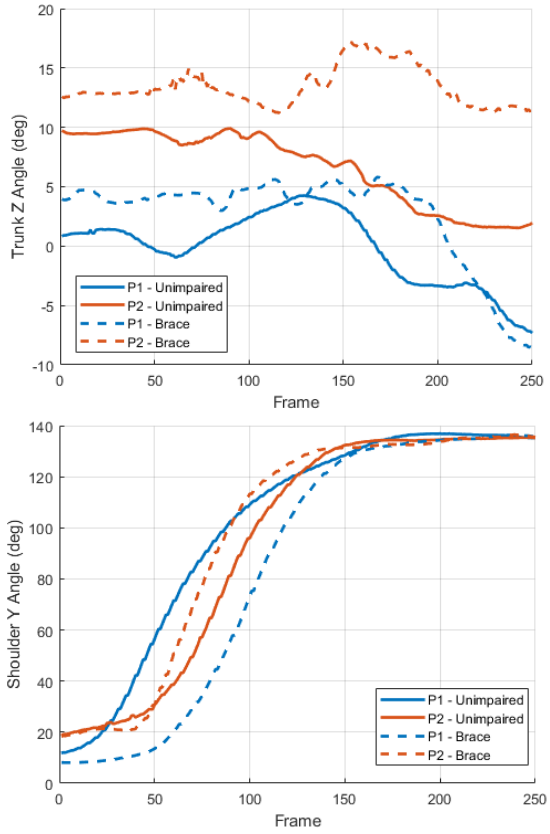

Figure 6. Two joint trajectories for participants P1 and P2 while reaching to target 9 (top plot) and target 1 (bottom plot) from Fig. 5. (Top) The trunk Z trajectories have clearly different ROM. (Bottom) The shoulder Y trajectories have similar start and end points which are also the maximum and minimum values. This would lead to similar ROM measurements, despite the motion patterns being different around the center of motion.

1) Difference in Range of Motion (dROM)

As discussed in Section 2, past studies on body compensation have examined joint ROM as an indicator of body compensation. We take a similar approach in our first metric by measuring range of motion for all joints in unimpaired and impaired (wearing the arm brace) cases, while also considering the difference in joint ROM between the cases.

ROM is calculated for each joint θ_n (n=1 to 10) for unimpaired (R_{Un}) and impaired (R_{Bn}) cases:

$$R_{Un} = \max(\theta_{Un}) - \min(\theta_{Un})$$

$$R_{Bn} = \max(\theta_{Bn}) - \min(\theta_{Bn})$$

The difference is then determined.

$$dROM_n = R_{Un} - R_{Bn}$$

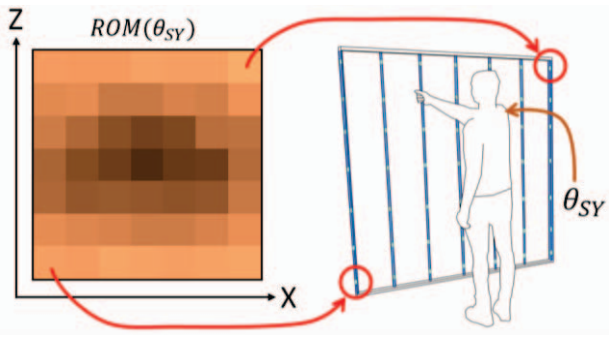

Figure 7. Metrics are represented as 'heat maps', with each square corresponding to joint/body segment behavior while reaching to a spatially equivilant target location on the grid (as viewed from the perspective of the participant). In this example, θ_{SY} refers to shoulder elevation angle while the heat map displays ROM (range of motion).

2) Cartesian Trajectory Length Analysis

It was hypothesized that variations in joint motion associated with compensatory movements may result in excessive motion of body segments in Cartesian space. Indeed, the elevation of the elbow is often observed as a compensatory motion in those with limited wrist mobility [5]. It is likely then that the path the elbow traces to reach this pose differs in length from the unimpaired configuration. As such, we propose measuring the Cartesian motion path length of various body segments as the sum of Euclidean distances between body segment positions in the motion data, (X_i, Y_i, Z_i) and $(X_{i+1}, Y_{i+1}, Z_{i+1})$:

$$L_{Un} = \sum_{i=0}^{l} \sqrt{|X_{Ui} - X_{Ui+1}|^2 + |Y_{Ui} - Y_{Ui+1}|^2 + |Z_{Ui} - Z_{Ui+1}|^2}$$

Where l is the number of samples in a targets' reaching trajectory and i is the current sample. This metric is calculated for the unimpaired (L_U) and impaired (braced) (L_B) trajectories. The difference is also calculated.

$$L_n = L_{Un} - L_{Bn}$$

V. Results

A total of 392 reaching motions were recorded, which also captured the joint variables and body segments listed in Table 2. The metrics discussed in Section IV were applied to these variables and have been visualized via spatially relevant heat maps, using the Matlab command *imagesc*. In these plots, each grid square represents motion associated with reaching to the corresponding grid target, as 'viewed' from the perspective of the participant (Fig 7). A mean result, $\bar{P}$, was also calculated by taking the average of corresponding array value across participants. The spatial nature of the data enables visual correlations to be made between the participants and mean result. We apologize that due to the necessary figure size, it has not been possible to place plots on the same page as their first mention in the text.

Table 2. Joint angle and body segment nomenclature. Shaded wrist angles have their motion restricted in the impaired test condition.

Trunk		Shoulder		Body Segments	
θ_{TX}	Flexion	θ_{SX}	Plane of Elevation	C_{Th}	Thorax Center
θ_{TY}	Rotation	θ_{SY}	Elevation	C_{Sh}	Shoulder Center
θ_{TZ}	Lateral Flexion	θ_{SZ}	Internal Rotation	C_{El}	Elbow Center
Elbow		**Wrist**		C_{Wr}	Wrist Center
θ_{EL}	Elbow Flexion	θ_{WX}	Pronation/Suppination		
		θ_{WY}	Flexion / Extension		
		θ_{WZ}	Radial/Ulnar Deviation		

Fig 8 illustrates the ROM for all measured joint angles in impaired and unimpaired condition in addition to the difference in ROM (dROM). These joint angles were determined from ISB standards [16] and are listed in Table 2 along with body segments used in the Cartesian trajectory length metric.

These results indicate patterns of spatial motion distribution which are fairly consistent between participants in both unimpaired and impaired cases. For example, the radial pattern of (θ_{SY}) indicates that participants typically increase their shoulder elevation ROM around the periphery of the workspace, rather than the center. Other distinct patterns are that elbow ROM increases in the lower portion of the workspace while θ_{TX} increases in the upper portion. θ_{TY} and θ_{TZ} are large in opposing quadrants. θ_{SX} and θ_{SY} are high throughout the workspace. The dROM results do not immediately visually indicate consistent patterns of ROM difference between participants, though further statistical analysis will later be applied to confirm this.

Fig 9 shows the Cartesian trajectory length of the four body segments described in Table 2. As in Fig 8, this has been indicated for unimpaired, impaired and the difference. As can be expected, trajectory length increases as participants reach across their body, to targets on the opposite side from their dominant limb. Differences in trajectory length follow this trend, with more variation away from the dominant side. Interestingly, the change seems quite balanced between length increase and decrease. It is also interesting to note that metric patterns are similar across multiple body segments for each participant, but show less similarity between participants.

A. Statistical Analysis

Though visual observations regarding patterns of motion may be made from the Figs 8-9, we wished to implement statistical measures to quantify trends.

Table 3 illustrates paired t-tests to determine if significant $(p<0.05)$ statistical differences exist between ROM for unimpaired and impaired motions for the same subject (Fig 8).

Significant motion differences are obviously unanimous for all the wrist DOF, which were subject to motion limitation. For other joints, shoulder elevation θ_{SY} and shoulder plane of elevation θ_{SX} show near unanimous significance. Shoulder

Table 3. Paired t-test p-values for comparing unimpaired and impaired ROM (Fig. 8). Shaded cells indicate $p<0.05$, which implies significant difference between unimpaired and impaired reaching patterns.

	θ_{TX}	θ_{TY}	θ_{TZ}	θ_{SX}	θ_{SY}	θ_{SZ}	θ_{EL}
P1	0.191	0.066	0.533	$1.31\text{x}10^{-7}$	$5.4\text{x}10^{-5}$	$6.81\text{x}10^{-10}$	$4.16\text{x}10^{-6}$
P2	0.067	$2.9\text{x}10^{-3}$	0.482	$6.51\text{x}10^{-7}$	0.062	0.048	$1.26\text{x}10^{-3}$
P3	0.318	0.711	0.751	$1.47\text{x}10^{-9}$	$4.94\text{x}10^{-11}$	0.886	0.06
P4	$3.51\text{x}10^{-4}$	0.049	0.729	0.197	$2.61\text{x}10^{-10}$	0.156	0.75
$\bar{P}$	0.263	0.100	0.465	$3.01\text{x}10^{-5}$	$1.24\text{x}10^{-13}$	$6.05\text{x}10^{-8}$	$2.44\text{x}10^{-4}$

	θ_{WX}	θ_{WY}	θ_{WZ}
P1	$4.03\text{x}10^{-18}$	$4.74\text{x}10^{-29}$	$1.26\text{x}10^{-22}$
P2	$6.11\text{x}10^{-10}$	$7.06\text{x}10^{-23}$	$3.24\text{x}10^{-26}$
P3	$7.07\text{x}10^{-14}$	$1.47\text{x}10^{-26}$	$2.48\text{x}10^{-19}$
P4	$3.51\text{x}10^{-4}$	$1.96\text{x}10^{-27}$	$3\text{x}10^{-19}$
$\bar{P}$	$1.54\text{x}10^{-23}$	$2.94\text{x}10^{-32}$	$4.63\text{x}10^{-32}$

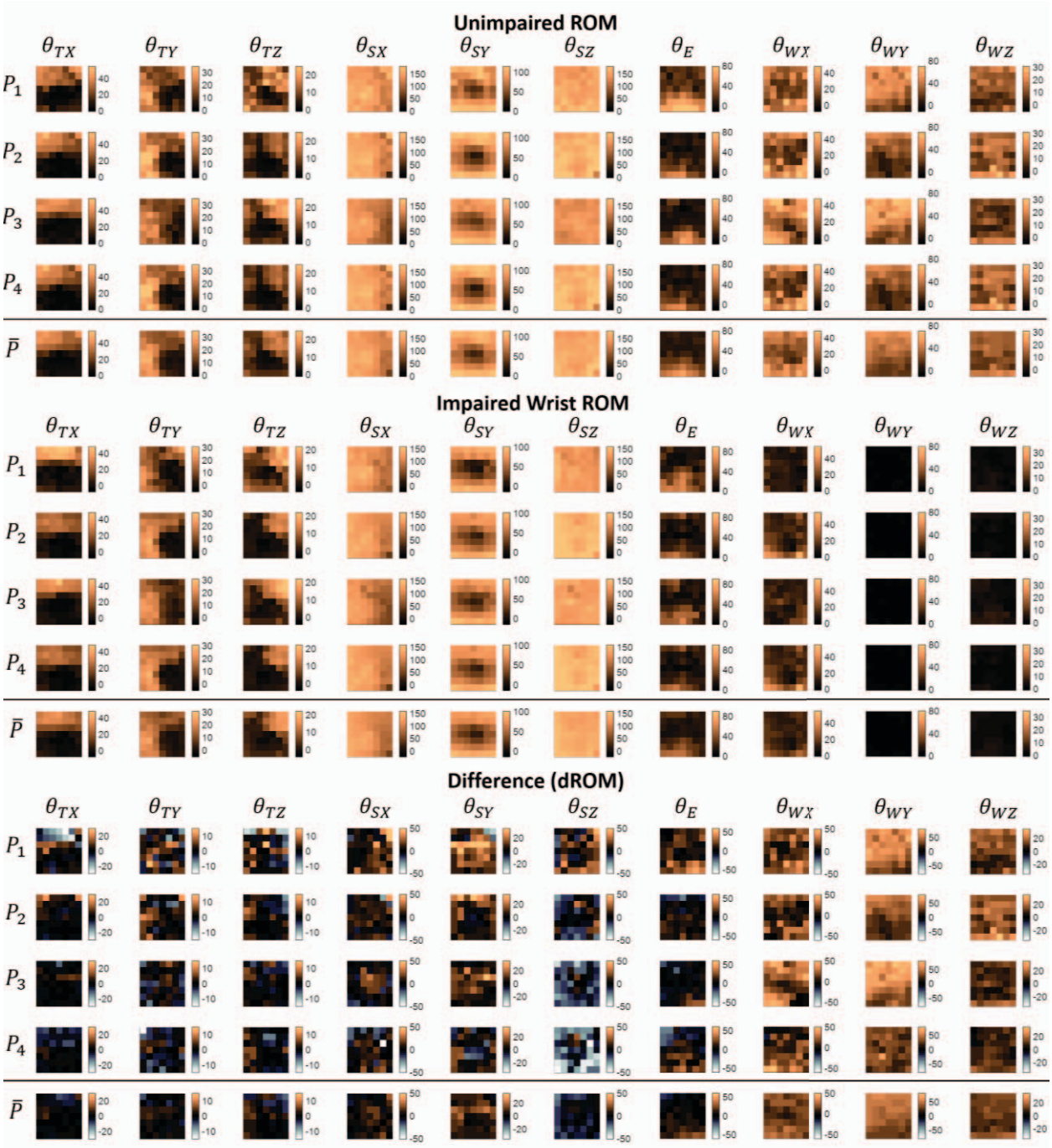

Figure 8. Range of Motion (ROM) for each joint during unimpaired reaching, impaired reaching and the difference between the two (dROM). Lighter colors in the Unimpaired and Impaired cases correspond to greater range of motion. In the dROM case darker colors are close to zero, and therefore indicate little difference, with lighter colors also indicating magnitude and sign of dROM, i.e. whether the difference resulted in greater (copper) or less (white) ROM. Note that the joints have the same color scale for both impaired and unimpaired ROM cases, though this is different in the dROM case.

internal rotation and elbow motion show significance in half of participants and the mean. The trunk DOF have the least significant differences.

Table 4 illustrates the same method of paired t-tests for Cartesian trajectory length of the four body segments. The results show that the elbow and wrist trajectories underwent a significant length change, with slightly more occurrence in the elbow. This matches the hypothesis of Section IV.2. The trajectory of the thorax and shoulder did not undergo a significant length change.

Table 4: Paired t-tests for Cartesian trajectory length of body segments

	C_{TH}	C_{Sh}	C_{El}	C_{Wr}
P1	0.409	0.515	$1.98\text{x}10^{-2}$	0.460
P2	0.869	0.058	$4.98\text{x}10^{-4}$	$2.25\text{x}10^{-3}$
P3	0.004	0.002	$4.81\text{x}10^{-5}$	$4.3\text{x}10^{-4}$
P4	0.340	0.512	0.412	0.774
$\bar{P}$	0.898	0.381	$9.27\text{x}10^{-3}$	$9.08\text{x}10^{-3}$

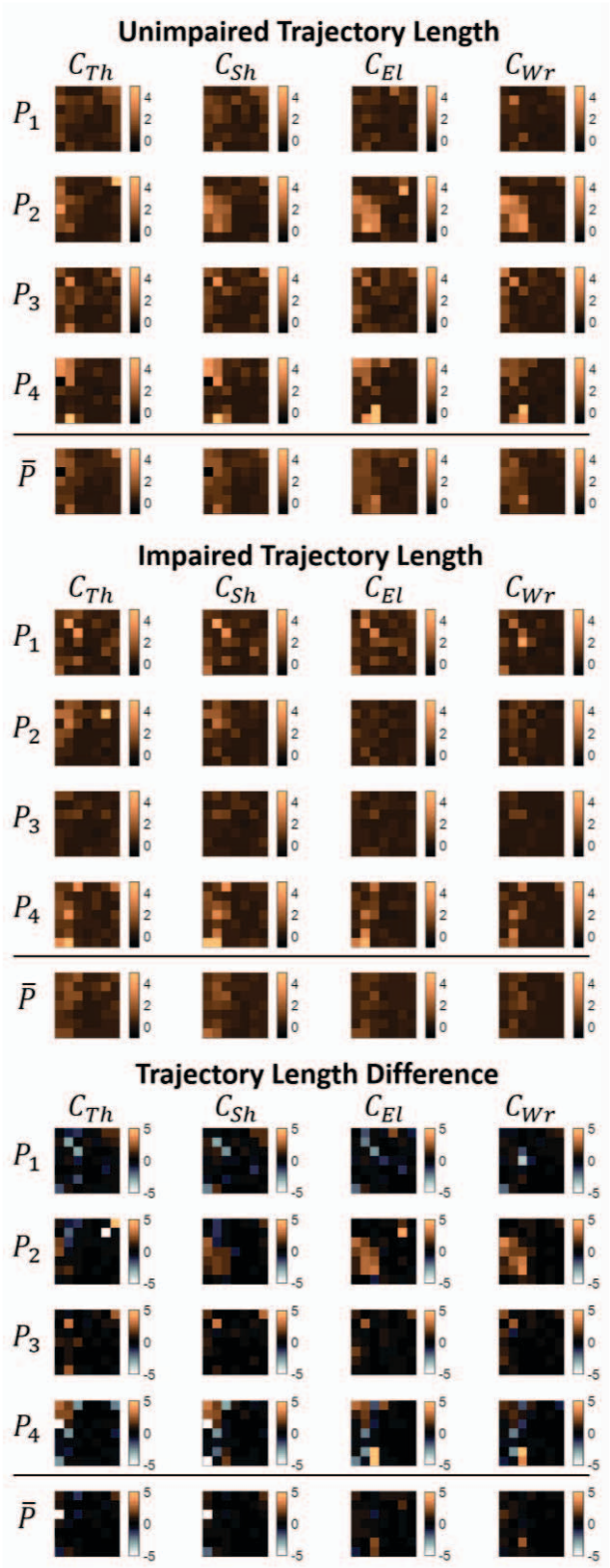

Figure 9. Cartesian path length metric for the thorax, shoulder center, elbow center and wrist center. Units are cm.

A second statistical measure was implemented to determine if spatial patterns of reaching motion were consistent between the four subjects for different variables, metrics and conditions. This comparison necessitates preserving the spatial grid structure of the data, to allow comparison of workspace behavior. This then excludes the use of common tools like ANOVA. Instead, a linear mixed effects model was fit to the data, using the Matlab command *fitlme*.

For each variable to be tested (e.g. dROM for Trunk Angle θ_{TX} from Fig 8), the response variable of model was defined as the array of mean participant metric results (e.g. the arrays illustrated by $\bar{P}$ in Fig 8-9), while input data was individual participant arrays for each metric.

If participants provide a similar response to a metric, then we expect a slope of 1, when assessing the relationship between the mean across participants ($\bar{P}$) and each participant (P_1-P_4). We accommodated a linear mixed effects model for each metric's variables where we use each participant as a random effect and fixed the intercept to 0. Here, our null hypothesis is that participants behave similarly, and thus the slope is 1; if rejected, then the participants are statistically different. A Gaussian cumulative distribution function was used with the model estimates to calculate a p-value, where ($p<0.05$) rejects the null hypotheses. These p-values for all variables in all metrics are shown in Table 5 and 6, where values of ($p\geq0.05$) have been highlighted to indicate the data shows a comparable pattern across participants.

Table 5 indicates that participant ROM patterns across the workspace were similar for all trunk and shoulder joints in the unimpaired and impaired cases. The value of dROM is naturally signed (Section IV.C.1), though we have also provided an unsigned value in Table 5, to examine difference magnitude but not direction. Interestingly, the similarities observed for the trunk and shoulder in the unimpaired and impaired cases are less pronounced in the dROM cases.

Though this may seem counter-intuitive, visual inspection of Fig 8 confirms that though the spatial patterns of unimpaired and impaired reaching are similar, there are subtle and seemingly unpredictable variations across participants.

Table 6 provides a linear mixed effects model approach for the Cartesian trajectory length data. Interestingly, in Table 6 we observe similarity only in the impaired, braced condition, implying that individuals had similar strategies for dealing with the loss of wrist motion, though as Fig 9 illustrates, this was through via both increasing and decreasing Cartesian trajectory length for different parts of the workspace.

Indeed, though human motion is optimized to some quantity, it is rarely a straight line when motion against gravity is involved [10]. The emergent compensation away

Table 5. Statistical measure of similarity between participant ROM data using a linear mixed effects model. Variables where $p\geq0.05$ (indicating correlation between participant movement patterns) have been shaded.

	θ_{TX}	θ_{TY}	θ_{TZ}	θ_{SX}	θ_{SY}	θ_{SZ}
Unimpaired	0.638	0.884	0.830	0.947	0.135	0.996
Impaired	0.812	0.788	0.939	0.998	0.188	0.956
dROM	$5.88\text{x}10^{-131}$	$4.67\text{x}10^{-151}$	$5.63\text{x}10^{-50}$	$2.32\text{x}10^{-63}$	$8.67\text{x}10^{-54}$	$1.23\text{x}10^{-128}$
|dROM|	0.225	$1.75\text{x}10^{-17}$	0.005	$9.39\text{x}10^{-21}$	0.053	0.150

	θ_{EL}	θ_{WX}	θ_{WY}	θ_{WZ}
Unimpaired	0.711	$7.42\text{x}10^{-6}$	0.934	0.799
Impaired	$1.71\text{x}10^{-9}$	0.627	$3.75\text{x}10^{-5}$	0.658
dROM	$6.68\text{x}10^{-46}$	$1.64\text{x}10^{-19}$	0.950	0.713
|dROM|	0.081	$1.24\text{x}10^{-14}$	0.950	0.737

Table 6. Statistical measure of similarity between participant ROM data using a linear mixed effects model. Variables where $p \geq 0.05$ (indicating correlation between participant movement patterns) have been shaded.

	C_{TH}	C_{Sh}	C_{El}	C_{Wr}
Unimpaired	0.005	0.003	0.072	0.010
Impaired	0.211	0.067	0.244	0.070
L_n	$1.1\text{x}10^{-129}$	$1.4\text{x}10^{-139}$	$1.97\text{x}10^{-136}$	$2.26\text{x}10^{-103}$
$\lvert L_n \rvert$	$8.05\text{x}10^{-30}$	$9.15\text{x}10^{-22}$	$3.15\text{x}10^{-44}$	$7.87\text{x}10^{-30}$

from these non-linear trajectories may therefore be difficult to predict and non-consistent across various individuals.

VI. Conclusion

This paper has proposed the extension of compensatory motion investigations beyond isolated activities of daily living and into discretely sampled workspaces. The dense resulting data has been displayed via a novel method that allows visual comparison of the effect of target location on various metrics. In addition to the standard measure of joint ROM, we have also measured Euclidean path length of four body segments in Cartesian space. The results visually indicated how regions of the workspace influence individual joint ROM, joint-level trajectories or Cartesian path changes when the user is moving naturally, or when wrist motion is impaired in 2DOFs. Though clear ROM and Euclidean patterns are present for un/impaired reaching motions (showing gradual metric change throughout the workspace), the difference metrics provides less clear spatial patterns, with limited observable similarity between participants.

Statistical approaches (Tables 4-7) were implemented to quantify, unimpaired/impaired variable differences and correlation between participants. Significant ROM changes were identified for all joints except the trunk. Significant Cartesian trajectory length changes occurred for the elbow and wrist, which matched general observations of wrist-less prosthetic user behavior. Measures of similarity across participants showed consistent ROM for the trunk and shoulder in impaired and unimpaired cases though this was less so for the compensatory (dROM) cases. In terms of Cartesian length, participants seemed to show similar braced motion strategies but were uncorrelated otherwise. The general trend of correlation in un/impaired cases but not in compensation (difference) is interesting and unexpected. It seems that though participants have comparable reaching strategies, the differences between these strategies is subject to some noise (θ_{SY} in Fig 8 is a clear example).

These initial findings indicate the value of spatial workspace sampling, as metrics change considerably depending on workspace location. The typical approach of measuring body compensation for a task at single location may lead an investigator or therapist to overlook varied data in neighboring locations.

Secondly the impact of increasing wrist mobility (via interventions such as rehabilitation, surgery or prosthetic devices) on reducing gross changes in joint ROM and trajectory length have been shown. The results may also be used in guiding therapists in understanding which areas of the workspace has the most motion demands on different aspects of the body.

Acknowledgment

We thank Ignacio Quintero from Yale University Statistics Department for insightful statistical advice.

References

[1] J. T. Belter, J. L. Segil, A. M. Dollar, and R. F. Weir, "Mechanical design and performance specifications of anthropomorphic prosthetic hands: A review," *J Rehabil Res Dev*, vol. 50, no. 5, p. 599, 2013.

[2] J. Zuniga, D. Katsavelis, J. Peck, J. Stollberg, M. Petrykowski, A. Carson, and C. Fernandez, "Cyborg beast: a low-cost 3d-printed prosthetic hand for children with upper-limb differences.," *BMC Res Notes*, vol. 8, no. 1, p. 10, 2015.

[3] N. M. Bajaj, A. J. Spiers, and A. M. Dollar, "State of the art in prosthetic wrists: Commercial and research devices," *2015 IEEE Int Conf Rehabil Robot*, pp. 331–338, 2015.

[4] F. Montagnani, M. Controzzi, and C. Cipriani, "Is it Finger or Wrist Dexterity That is Missing in Current Hand Prostheses?," *IEEE Trans Neural Syst Rehabil Eng*, vol. 21, no. c, pp. 1–1, 2015.

[5] A. Hussaini, A. Zinck, and P. Kyberd, "Categorization of compensatory motions in transradial myoelectric prosthesis users," *Prosthet Orthot Int*, 2016.

[6] M. Deijs, R. M. Bongers, N. D. M. Ringeling-Van Leusen, and C. K. Van Der Sluis, "Flexible and static wrist units in upper limb prosthesis users: Functionality scores, user satisfaction and compensatory movements," *J Neuroeng Rehabil*, vol. 13, no. 1, 2016.

[7] A. Murgia, P. Kyberd, and T. Barnhill, "The use of kinematic and parametric information to highlight lack of movement and compensation in the upper extremities during activities of daily living," *Gait Posture*, vol. 31, no. 3, pp. 300–306, 2010.

[8] A. Spiers and G. Herrmann, "An optimal sliding mode controller applied to human motion synthesis with robotic implementation," in *American Control*, 2010.

[9] T. Kang, J. He, and S. I. H. Tillery, "Determining natural arm configuration along a reaching trajectory," *Exp Brain Res*, vol. 167, no. 3, pp. 352–361, 2005.

[10] A. Spiers, S. G. Khan, and G. Herrmann, *Biologically inspired control of humanoid robot arms: Robust and adaptive approaches*. 2016.

[11] M. J. Major, R. L. Stine, C. W. Heckathorne, S. Fatone, and S. a Gard, "Comparison of range-of-motion and variability in upper body movements between transradial prosthesis users and able-bodied controls when executing goal-oriented tasks.," *J Neuroeng Rehabil*, vol. 11, no. 1, 2014.

[12] S. L. Carey, M. Jason Highsmith, M. E. Maitland, and R. V Dubey, "Compensatory movements of transradial prosthesis users during common tasks.," *Clin Biomech (Bristol, Avon)*, vol. 23, no. 9, pp. 1128–35, Nov. 2008.

[13] B. D. Adams, N. M. Grosland, D. M. Murphy, and M. McCullough, "Impact of impaired wrist motion on hand and upper-extremity performance," *J Hand Surg Am*, vol. 28, no. 6, pp. 898–903, 2003.

[14] A. G. Mell, B. L. Childress, and R. E. Hughes, "The effect of wearing a wrist splint on shoulder kinematics during object manipulation.," *Arch Phys Med Rehabil*, vol. 86, no. 8, pp. 1661–4, Aug. 2005.

[15] C. M. Light, P. H. Chappell, and P. J. Kyberd, "Establishing a standardized clinical assessment tool of pathologic and prosthetic hand function: Normative data, reliability, and validity," *Arch Phys Med Rehabil*, vol. 83, no. 6, pp. 776–783, 2002.

[16] G. Wu, F. C. T. Van Der Helm, H. E. J. Veeger, M. Makhsous, P. Van Roy, C. Anglin, J. Nagels, A. R. Karduna, K. McQuade, X. Wang, F. W. Werner, and B. Buchholz, "ISB recommendation on definitions of joint coordinate systems of various joints for the reporting of human joint motion - Part II: Shoulder, elbow, wrist and hand," *J Biomech*, vol. 38, no. 5, pp. 981–992, 2005.